

Effects of CO₂ perturbation on phosphorus pool sizes

M. Nausch et al.

Effects of CO₂ perturbation on phosphorus pool sizes and uptake in a mesocosm experiment during a low productive summer season in the northern Baltic Sea

M. Nausch¹, L. Bach², J. Czerny², J. Goldstein^{1,a}, H. P. Grossart^{4,5},
D. Hellemann^{2,b}, T. Hornick⁴, E. Achterberg^{3,c}, K. Schulz², and U. Riebesell²

¹Leibniz Institute for Baltic Sea Research, Seestrasse 15, 18119 Rostock, Germany

²GEOMAR Helmholtz Centre for Ocean Research Kiel, Düsternbrooker Weg 20, 24105 Kiel, Germany

³Ocean and Earth Science, University of Southampton National Oceanography Centre Southampton, Southampton SO14 3ZH, UK

⁴Leibniz-Institute for Freshwater Ecology and Inland Fisheries, Zur alten Fischerhütte 2, 16775 Stechlin, Germany

⁵Potsdam University, Institute for Biochemistry and Biology, Maulbeerallee 2, 14469 Potsdam, Germany

Title Page

Abstract

Introduction

Conclusions

References

Tables

Figures

◀

▶

◀

▶

Back

Close

Full Screen / Esc

Printer-friendly Version

Interactive Discussion



^anow at: Max-Planck Odense Center on the Biodemography of Aging & Department of Biology, Campusvej 55, 5230 Odense M, Denmark

^bnow at: Department of Environmental Sciences, University of Helsinki, PL 65 00014 Helsinki, Finland

^cnow at: GEOMAR Helmholtz Centre for Ocean Research Kiel, Düsternbrooker Weg 20, 24105 Kiel, Germany

Received: 25 September 2015 – Accepted: 2 October 2015 – Published: 30 October 2015

Correspondence to: M. Nausch (monika.nausch@io-warnemuende.de)

Published by Copernicus Publications on behalf of the European Geosciences Union.

BGD

12, 17543–17593, 2015

Effects of CO₂ perturbation on phosphorus pool sizes

M. Nausch et al.

Title Page

Abstract

Introduction

Conclusions

References

Tables

Figures



Back

Close

Full Screen / Esc

Printer-friendly Version

Interactive Discussion



Abstract

Studies investigating the effect of increasing CO₂ levels on the phosphorus cycle in natural waters are lacking although phosphorus often controls phytoplankton development in aquatic systems. The aim of our study was to analyze effects of elevated CO₂ levels on phosphorus pool sizes and uptake. Therefore, we conducted a CO₂-manipulation mesocosm experiment in the Storfjärden (western Gulf of Finland, Baltic Sea) in summer 2012. We compared the phosphorus dynamics in different mesocosm treatments but also studied them outside the mesocosms in the surrounding fjord water.

In the mesocosms as well as in surface waters of Storfjärden, dissolved organic phosphorus (DOP) concentrations of 0.26 ± 0.03 and $0.23 \pm 0.04 \mu\text{molL}^{-1}$, respectively, formed the main fraction of the total P-pool (TP), whereas phosphate (PO₄) constituted the lowest fraction with mean concentration of $0.15 \pm 0.02 \mu\text{molL}^{-1}$ and $0.17 \pm 0.07 \mu\text{molL}^{-1}$ in the mesocosms and in the fjord, respectively. Uptake of PO₄ ranged between 0.6 and 3.9 nmolL⁻¹h⁻¹ of which ~86% (mesocosms) and ~72% (fjord) were realized by the size fraction < 3 μm. Adenosine triphosphate (ATP) uptake revealed that additional P was supplied from organic compounds accounting for 25–27% of P provided by PO₄ only.

CO₂ additions did not cause significant changes in phosphorus (P) pool sizes, DOP composition, and uptake of PO₄ and ATP when the whole study period was taken into account. About 18% of PO₄ was transformed into POP, whereby the major proportion (~82%) was converted into DOP suggesting that the conversion of PO₄ to DOP is the main pathway of the PO₄ turnover.

We observed that significant relationships (e.g., between POP and Chl *a*) in the untreated mesocosms vanished under increased *f*CO₂ conditions. Consequently, it can be hypothesized that the relationship between POP formation and phytoplankton growth changed under elevated CO₂ conditions. Significant short-term effects were observed for PO₄ and particulate organic phosphorus (POP) pool sizes in CO₂ treatments > 1000 μatm during periods when phytoplankton started to grow.

BGD

12, 17543–17593, 2015

Effects of CO₂ perturbation on phosphorus pool sizes

M. Nausch et al.

Title Page

Abstract

Introduction

Conclusions

References

Tables

Figures

◀

▶

◀

▶

Back

Close

Full Screen / Esc

Printer-friendly Version

Interactive Discussion



1 Introduction

Increasing emissions of anthropogenic CO₂ into the atmosphere and subsequent acidification of the ocean can potentially affect the diversity of organisms and the functioning of marine ecosystems (Eisler, 2011). The rise of the atmospheric CO₂ content was accelerated from 3.4±0.2PgCyr⁻¹ in the 1980s to 4.0±0.2PgCyr⁻¹ in the 2000s leading to CO₂ elevation in ocean surface waters the same rate (IPCC, 2013). Atmospheric CO₂ is predicted to rise to 750–> 1000ppm in 2100 (IPCC, 2001) corresponding with a decrease in pH by 0.3–0.5 units (Caldeira and Wickett, 2005) from the present pH of 8.1. Although this process is of global significance and all parts of the oceans are at risk, there will be regional differences in the degree of acidification (Borges et al., 2005). Thus, to determine the CO₂-related changes in the oceans, multiple studies in different regions are required. Semi-enclosed coastal regions, such as the Baltic Sea, can be more sensitive to CO₂ elevation than open ocean waters due to high freshwater inputs resulting in a reduced buffer capacity (Orr, 2011).

In the Baltic Sea, several studies of CO₂ effects are done on the organismic level of fish (Frommel et al., 2013), zooplankton (Pansch et al., 2012; Vehmaa et al., 2012), macrophytes (Pajusalu et al., 2013), benthic organisms (Hiebenthal et al., 2013; Stemmer et al., 2013), and filamentous cyanobacteria (Czerny et al., 2009; Eichner et al., 2014; Wannicke et al., 2012). The impacts of elevated CO₂ at the ecosystem level, however, have thus far been limited to the Kiel Bay in the western Baltic Sea (Engel et al., 2014; Rossoll et al., 2013; Schulz and Riebesell, 2013), which may fundamentally differ from other parts of the Baltic Sea.

Next to nitrogen, phosphorus (P) controls the productivity of phytoplankton in the ocean (Karl, 2000; Sanudo-Wilhelmy et al., 2001; Tyrrell, 1999) and is the limiting factor in some regions (Ammerman et al., 2003). The total phosphorus (TP) pool comprises phosphate (PO₄), dissolved organic phosphorus (DOP), and particulate organic phosphorus (POP). There is a continuous transformation of phosphorus between these P species due to their uptake, conversion, and release by organisms. While PO₄ is the

BGD

12, 17543–17593, 2015

Effects of CO₂ perturbation on phosphorus pool sizes

M. Nausch et al.

Title Page

Abstract

Introduction

Conclusions

References

Tables

Figures



Back

Close

Full Screen / Esc

Printer-friendly Version

Interactive Discussion



Effects of CO₂ perturbation on phosphorus pool sizes

M. Nausch et al.

Title Page

Abstract

Introduction

Conclusions

References

Tables

Figures



Back

Close

Full Screen / Esc

Printer-friendly Version

Interactive Discussion



ter depth of ~ 30 m. Only six of them were included throughout the whole study period since leakages in the remaining three rendered them unusable. Equipment and deployment procedures are described in detail by Paul et al. (2015b). Briefly, polyurethane enclosure bags of 2 m in diameter and 18.5 m in length were mounted in floating frames and lowered in such a way that ~ 17 m of each bag were immersed in the water column and ~ 1.5 m remained above the water surface. Large organisms were excluded from the mesocosms by a 3 mm mesh installed at the top and bottom of the bags before closure. The mesocosms were deployed 10 days prior to CO₂ manipulation to rinse the bags and for full water exchange. Sediment traps were mounted on the lower ends to close them water tight, while the upper ends were raised above the water surface to prevent water entry during wave action. The mesocosms were covered with a dome shaped roof to prevent nutrient input by bird and potentially significant fresh water input by rain. Salinity gradients were removed by bubbling the mesocosms with compressed air for 3.5 min, so that 5 days before the start of the experiment (day -5) the water body was fully homogeneous.

CO₂ treatment started on day 0 and was repeated on subsequent 4 days by pumping various quantities of 50 μ m-filtered and CO₂-enriched fjord water into seven of the mesocosms as described by Riebesell et al. (2013). The intended CO₂ and pH gradients were reached after the last treatment on day 4. Details are described in Paul et al. (2015b). For the two untreated (control) mesocosms, only filtered fjord water was added to adjust the water volume to that of the treated mesocosms. To compensate for outgassing, the CO₂ manipulation was similarly repeated in the upper 7 m layer of the mesocosms on day 16.

2.2 Sampling

Daily sample collection started 3 days before the first CO₂ injection (day -3). Parallel samples were taken from the surrounding fjord. Sampling over the entire 17 m depth was carried out using an integrating water sampler (IWS HYDROBIOS-KIEL) that was

lowered slowly on a cable by hand. The sampling frequency differed depending on the parameter to be observed as shown in the overview by Paul et al. (2015b).

Phosphorus pool parameters and uptake rates were determined every second day, except for dissolved organic phosphorus (DOP) components, which were measured every 4 days. Termination of the measurements varied due to logistical constraints. Thus, total phosphorus (TP) and DOP were sampled only until day 29 whereas other parameters were sampled until day 43.

The collected water was filled in HCl-cleaned polyethylene canisters that had been pre-rinsed with sample water. All containers were stored in the dark. Back on land, subsamples were processed immediately for each P-analysis. The other analyses were carried out within a few hours of sample collection and sample storage in a climate room at in situ temperature.

2.3 Analytical methods

2.3.1 Temperature, salinity, and carbonate chemistry

Measurements in the fjord and in each mesocosm were conducted using a CTD60M memory probe (Sea and sun technology, Trappenkamp, Germany) lowered from the surface to a depth of 17 m at about 0.3 m s^{-1} in the early afternoon (1:30–2:30 p.m.). For these parameters, the depth-integrated mean values are presented here.

The carbonate system is described in detail in Paul et al. (2015b). The pH was determined using the spectrophotometric method (Dickson et al., 2007) using a Cary 100 (Varian) spectro-photometer and the dye M-cresol as indicator. Extinction was measured at 578 nm (E1) and 434 nm (E2) in a 10 cm cuvette. The pH was calculated from the ratio of E1 and E2 (Clayton and Byrne, 1993).

DIC was measured using a colorimetric AIRICA system (MARIANDA, Kiel) measuring the infrared absorption after purging the sample and calibration with certified reference material (CRM; Dr. A. Dickson, University of California, San Diego).

BGD

12, 17543–17593, 2015

Effects of CO₂ perturbation on phosphorus pool sizes

M. Nausch et al.

Title Page

Abstract

Introduction

Conclusions

References

Tables

Figures

◀

▶

◀

▶

Back

Close

Full Screen / Esc

Printer-friendly Version

Interactive Discussion



A_T was determined using potentiometric titration and a Gran type data analysis following Dickson et al. (2007). The quality of the measurement was verified with the same reference material as used for the DIC measurements.

The $f\text{CO}_2$ was calculated from DIC, pH, salinity, temperature, phosphate, and silicate data using the CO_2 SYS program (Pierrot and Wallace, 2006).

2.3.2 Chlorophyll and inorganic nutrients

Subsamples of 500 mL were filtered onto GF/F-filters, which were then homogenized. Chl *a* was extracted in acetone (90%) in plastic vials by homogenisation of the filters for 5 min in a cell mill using glass beads. After centrifugation (10 min, $800 \times g$, 4°C) the supernatant was analysed on a fluorometer (TURNER 10-AU) at an excitation of 450 nm and an emission of 670 nm to determine Chl *a* concentrations (Jeffrey and Welschmeyer, 1997).

A segmented continuous-flow analyzer coupled with a liquid-waveguide capillary flow-cell (LWCC) of 2 m length was used to determine phosphate (PO_4) and the sum of nitrite and nitrate ($\text{NO}_2 + \text{NO}_3$) at nanomolar precision (Patey et al., 2008). The PO_4 determination was based on the molybdenum blue method of Murphy and Riley (1962), and $\text{NO}_2 + \text{NO}_3$ on the method of Morris and Riley (1963). PO_4 concentrations from the same subsample were also measured manually using a 5 cm cuvette (Grasshoff et al., 1983). In most of the samplings PO_4 data obtained from both methods did not differ significantly (paired t test: $p = 0.0262$, $t = 1.127$, $n = 109$).

2.3.3 Dissolved organic phosphorus (DOP)

For the determination of DOP, duplicate 40 mL subsamples were filtered through pre-combusted (6 h, 450°C) glass fiber filters (Whatman GF/F) and stored in 50 mL vials (Falcon) at 20°C until further processing. The thawed samples were oxidized in a microwave (MARSXpress, CEM, Matthews, USA) after the addition of potassium peroxydisulfate in an alkaline medium (Grasshoff et al., 1983). The P concentration, measured

BGD

12, 17543–17593, 2015

Effects of CO_2 perturbation on phosphorus pool sizes

M. Nausch et al.

Title Page

Abstract

Introduction

Conclusions

References

Tables

Figures

◀

▶

◀

▶

Back

Close

Full Screen / Esc

Printer-friendly Version

Interactive Discussion



A2383) ranging from 1 to 20 nmolL⁻¹. The detection limit of the bioluminescence assay was 2.5 pmol mL⁻¹. The fluorescence slope of the standard concentrations was used to calculate dATP concentrations, correcting for the final sample volume. The P-content of the ATP (ATP-P) was calculated by assuming that 1 mol of ATP is equivalent to 3 mol P.

Dissolved phospholipids

The phosphate content of the dissolved phospholipids (PL-P) was analyzed using a modified method of Suzumura and Ingall (2001, 2004). Briefly, 400 mL subsamples of the filtrate were stored at -20 °C until further processing. The samples were then thawed in a water bath at 30 °C and extracted twice with 100 mL of chloroform. The chloroform phase was collected, concentrated to 5 mL in a rotary evaporator (Heidolph Instruments, Schwabach, Germany), and then transferred into microwave tubes. The chloroform was completely evaporated by incubating the tubes in a 60 °C water bath overnight. After the addition of 20 mL of deionized water (Milli-Q, Millipore), the samples were digested with potassium peroxydisulfate in alkaline medium and microwaved as described for the DOP analysis. Six standard concentrations of phospholipids, ranging from 0 to 125 µg L⁻¹, were prepared by adding the respective amounts of a stock solution containing 5 mg of l-phosphatidyl-dl-glycerol sodium salt (PG, Sigma Aldrich, P8318) mL⁻¹ to the aged seawater. The detection limit was 0.8 nmol L⁻¹. The blanks contained only chloroform and were processed as for the samples.

Dissolved DNA and RNA

Dissolved DNA and RNA (dDNA and dRNA) concentrations were determined according to Karl and Bailiff (1989) and as described by Unger et al. (2013). For each sample, 200 mL of the filtrate was gently mixed with the same volume of ethylene-diamine-tetracetic acid (EDTA, 0.1 M, pH 9.3, Merck, 1.08454) and 4 mL of cetyltrimethyl-ammonium bromide (CTAB, Sigma-Aldrich, H5882) and stored frozen at -20 °C for

BGD

12, 17543–17593, 2015

Effects of CO₂ perturbation on phosphorus pool sizes

M. Nausch et al.

Title Page

Abstract

Introduction

Conclusions

References

Tables

Figures

◀

▶

◀

▶

Back

Close

Full Screen / Esc

Printer-friendly Version

Interactive Discussion



Particulate carbon (PC) and nitrogen (PN) were analyzed by filtering 500 mL samples onto pre-combusted (450 °C, 6 h) glass fiber filters (Whatman GF/F), which were then stored frozen at -20 °C. PC and PN concentrations were measured by flash combustion of the dried (60 °C) filters using an EuroEA elemental analyser coupled with a Conflo II interface to a Finnigan Delta^{Plus} mass spectrometer.

2.3.6 Phosphate and ATP uptake

PO₄ uptake was measured by addition of radioactively labeled phosphate [³³P]PO₄ (specific activity of 111 TBqmmol⁻¹, Hartmann Analytic GmbH) at concentrations of 50 pmolL⁻¹ to 50 mL subsamples, which were then incubated under laboratory light and the in situ temperatures for ~ 2 h. For each mesocosm, three parallel samples and a blank were prepared. The blank was obtained by the addition of formaldehyde (1 % final concentration) 10 min before radiotracer addition, in order to poison the samples. At defined time intervals within the incubation, 5 mL subsamples were taken from each of the parallel samples and filtered onto polycarbonate filters pre-soaked with a cold 20 mM PO₄ solution to prevent non-specific [³³P]PO₄ binding. The filters were rinsed with 5 times 1 mL of particle-free bay water and placed in 6 mL scintillation vials. Scintillation liquid (4 mL IrgaSafe; Perkin Elmer) was added and the contents of the vials were mixed using a vortex mixer. After allowing the samples to stand for at least 2 h, the radioactivity on the filters was counted in a Perkin Elmer scintillation counter. Filters of 0.2 and 3 μm pore sizes (Whatman and Millipore, respectively) were used to determine uptake by the whole plankton community and the size fraction > 3 μm, respectively. Picoplankton uptake was calculated as the difference between the activity on the 0.2 μm and 3 μm filters.

[γ³³P]ATP (specific activity of 111 TBqmmol⁻¹, Hartmann Analytic GmbH) was added to triplicate 10 mL samples and a blank, each in a 20 mL vial, at a concentration of 50 pmolL⁻¹. The samples were incubated in the dark at in situ temperature for 1 h. The uptake was stopped by addition of 200 μL of a cold 20 mM ATP solution to

BGD

12, 17543–17593, 2015

Effects of CO₂ perturbation on phosphorus pool sizes

M. Nausch et al.

Title Page

Abstract

Introduction

Conclusions

References

Tables

Figures

⏪

⏩

◀

▶

Back

Close

Full Screen / Esc

Printer-friendly Version

Interactive Discussion



the samples, which were then filtered and processed as described for the PO₄ uptake measurements.

2.3.7 Bacterial production (BPP)

Rates of bacterial protein production (BPP) were determined by incorporation of ¹⁴[C]-leucine (¹⁴C-Leu, Simon and Azam, 1989) according to Grossart et al. (2006). Triplicates and a formalin-killed control were incubated with ¹⁴C-Leu (213 mCi mmol⁻¹; Hartmann Analytic GmbH, Germany) at a final concentration of 165 nmol L⁻¹, which ensured saturation of uptake systems of both free and particle-associated bacteria. Incubation was performed in the dark at in situ temperature (between 7.8 °C and 15.8 °C) for 1.5 h. After fixation with 2 % formalin, samples were filtered onto 5.0 μm (attached bacteria) nitrocellulose filters (Sartorius, Germany) and extracted with ice-cold 5 % trichloroacetic acid (TCA) for 5 min. Thereafter, filters were rinsed twice with ice-cold 5 % TCA, once with ethanol (96 % v/v), and dissolved with ethylacetate for measurement by liquid scintillation counting. Afterwards the collected filtrate was filtered on 0.2 μm (free-living bacteria) nitrocellulose filters (Sartorius, Germany) and processed in the same way as the 5.0 μm filters. Standard deviation of triplicate measurements was usually < 15 %. The sum of both fractions (free-living bacteria and attached bacteria) is referred to total BPP. The amount of incorporated ¹⁴C-Leu was converted into BPP by using an intracellular isotope dilution factor of 2. A conversion factor of 0.86 was used to convert the protein produced into carbon (Simon and Azam, 1989).

2.3.8 Statistical analyses

The Grubbs test, done online (graphpad.com/quickcalcs/Grubbs1.cfm) was applied to identify outliers in all data sets. The outliers were removed from further statistical analyses.

Effects of CO₂ perturbation on phosphorus pool sizes

M. Nausch et al.

Title Page

Abstract

Introduction

Conclusions

References

Tables

Figures

◀

▶

◀

▶

Back

Close

Full Screen / Esc

Printer-friendly Version

Interactive Discussion



Spearman Rank correlations were carried out to describe the relationship between the development of the parameters over time in the mesocosms and in the fjord using Statistica 6 software.

Short-term CO₂ effects on POP concentrations at days 0–2 and 23–43 between the CO₂ treatments were verified with an ANCOVA analysis using the SPSS software. The “days” were treated as a covariate interacting with the treatments. Paired *t* test was applied to check the differences in PO₄ concentrations between the treatments.

3 Results

3.1 Development in the mesocosms

3.1.1 CO₂, pH, temperature and salinity

The different mesocosms were characterized based on their averaged *f*CO₂ and pH values from day 1 until day 43 (Fig. 2a and b):

M1 and M5: 365 and 368 μmolL⁻¹ *f*CO₂, pH 8.08 and 8.07 untreated levels;

M7 and M6: 497 and 821 μmolL⁻¹ *f*CO₂, pH 7.95 and 7.74 intermediate *f*CO₂;

M3 and M8: 1007 and 1231 μmolL⁻¹ *f*CO₂, pH 7.66 and 7.58 high *f*CO₂.

Temperature development in the mesocosms was determined through temperature variations in the fjord from 7.81 to 15.86 °C. Based on this, the experiment was divided into four phases (Fig. 3): phase 0: day –3 to day 0; phase I: days 1–16, phase II: days 17–30 and phase III: day 31 until the end of the measurements. Temperature dropped from 8.71 to 7.82 °C in phase 0 and rose from 8.07 °C at the end of phase 0 to the maximum of 15.86 °C by the end of phase I. During phase II, the temperature decreased to 7.89 °C interrupted by a short reversal on days 22 and 23. During phase III, the temperature increased to 12.61 °C (Table 1).

The salinity of 5.69 ± 0.01 remained relatively stable in the mesocosms throughout the entire experimental period (Fig. 3).

BGD

12, 17543–17593, 2015

Effects of CO₂ perturbation on phosphorus pool sizes

M. Nausch et al.

Title Page

Abstract

Introduction

Conclusions

References

Tables

Figures

◀

▶

◀

▶

Back

Close

Full Screen / Esc

Printer-friendly Version

Interactive Discussion



3.1.2 Phytoplankton biomass

Chlorophyll *a* (Chl *a*) reached maximum concentrations of 2.06–2.48 $\mu\text{g L}^{-1}$ at day 5 (Fig. 4). Average concentrations of $1.94 \pm 0.23 \mu\text{g L}^{-1}$ in phase I exceeded those in phases II and III when Chl *a* decreased to a mean of $1.08 \pm 0.16 \mu\text{g L}^{-1}$. The increase in Chl *a* in the high CO_2 mesocosms by 24% in phase III was statistically significant (Paul et al., 2015b), and differences of $0.27 \mu\text{g L}^{-1}$ were only marginal.

We observed a significant relationship between Chl *a* and PO_4 in the untreated and intermediate treated mesocosms that was diminished with increasing $f\text{CO}_2$ indicated by lower p values. The significance got lost in the highest $f\text{CO}_2$ mesocosms (Table 2).

3.1.3 Phosphorus Pools

Total phosphorus (TP) concentrations in the mesocosms ranged between 0.49 and $0.68 \mu\text{mol L}^{-1}$ (Fig. 5a) without significant differences between the different CO_2 treatments. Shortly after the bags were closed, the decline in TP concentrations began and continued until the beginning of phase II. On average, TP concentrations decreased from $0.63 \pm 0.02 \mu\text{mol L}^{-1}$ on day -3 to $0.51 \pm 0.01 \mu\text{mol L}^{-1}$ on day 21. Thereafter, the mean TP remained constant at $0.54 \pm 0.03 \mu\text{mol L}^{-1}$ until the end of the measurements. Thus, the loss of phosphorus (116 nmol L^{-1}) from the 17 m layer during the 29 day measurement period was calculated to be $4.0 \text{ nmol L}^{-1} \text{ day}^{-1}$. The decline in TP can be explained by loss through sedimentation of POP (Paul et al., 2015b).

Particulate organic phosphorus (POP) concentrations varied from 0.10 to $0.23 \mu\text{mol L}^{-1}$ in all CO_2 treatments (Figs. 5b and 6). We expected that the decrease in TP was reflected in POP. However, parallel changes occurred only periodically. POP concentrations increased during the first 5 days after the bags were closed. This increase was stimulated by the CO_2 treatments from day 0 to day 2 (ANCOVA: $p = 0.004$, $F = 20.811$) (Fig. 7a). Subsequently, POP declined in parallel with TP until day 21, albeit with a lower amount. Averaged over all mesocosms, TP decreased by $0.12 \mu\text{mol L}^{-1}$, whereas POP declined only by $0.06 \mu\text{mol L}^{-1}$ during this period. From

3.2.3 Phosphorus-Pools

TP concentrations from day -3 until day 29 ranged between 0.54 and 0.70 μmolL^{-1} (mean $0.61 \pm 0.04 \mu\text{molL}^{-1}$; $n = 19$) (Figs. 5a and 6a). The progression of TP differed from that of the hydrographic parameters or the Chl *a* concentrations. With a general decreasing tendency, TP undulated with a frequency of about 10 days in the period of phases 0 to the first half of phase I and of 6 days in the second half of phase I to II. For the period under investigation, the TP fractions had the following characteristics:

POP concentrations varied from 0.13 to 0.30 μmolL^{-1} (mean $0.20 \pm 0.04 \mu\text{molL}^{-1}$; $n = 29$), thus accounting for 23.4–51.8% (mean $34.7 \pm 7.9\%$; $n = 19$) of the TP pool. The development of POP over time did not follow that of TP (Fig. 6b). POP concentrations were highest between days 8 and 19, when the accumulation of POP in the biomass was reflected in declining C : P ratios from 180 to 107 and thereafter remained at the low ratio until the end of the measurements. The POP increase in phase III occurred in parallel to Chl *a* and to the PO_4 decrease (Table 5). Thus PO_4 was transformed into POP via biomass production. The calculated P content of phytoplankton was 0.05–0.15 (mean 0.1) $\mu\text{mol POP} (\mu\text{g Chl } a)^{-1}$.

DOP substantially contributed (26–45%) to the TP pool (Fig. 6). Concentrations ranged between 0.19 and 0.29 μmolL^{-1} (mean $0.24 \pm 0.03 \mu\text{molL}^{-1}$; $n = 17$), with high concentrations occurring in parallel to those of TP in phases I and II (Fig. 5c). The very low DOP value of 0.11 μmolL^{-1} , on day 29, was an outlier (Grubbs test) and was excluded from the calculation. For the whole study period, DOP concentrations correlated positively with both POP and PO_4 turnover times and inversely with PO_4 concentrations (Table 5). A similar behavior between DOP and Chl *a* was restricted to phases 0 and I, whereas the relationship was inverse in phase II (Fig. 8b) indicating that upwelling of deep water did not change the DOP concentrations in surface water. As shown in Fig. 8a, the DOP and BPP levels alternated with the same rhythm, but inversely, in phases 0 and I and changed to a parallel development in phase II. Statistical analysis

BGD

12, 17543–17593, 2015

Effects of CO_2 perturbation on phosphorus pool sizes

M. Nausch et al.

Title Page

Abstract

Introduction

Conclusions

References

Tables

Figures

◀

▶

◀

▶

Back

Close

Full Screen / Esc

Printer-friendly Version

Interactive Discussion



was not feasible because DOP and BPP were not always sampled on the same day and only very few data pairs were available.

Phosphorus, derived from the sum of ATP, PL, RNA, and DNA, constituted 42.8–72.0% (mean $59.7 \pm 10.7\%$; $n = 7$) of the DOP pool (Table 3). Thus, 27.8–57.2% of the DOP remained unidentified. Concentrations of $1.4\text{--}4.6\text{ nmol ATP L}^{-1}$, $0.6\text{--}4.5\text{ nmol PLL}^{-1}$, $42.2\text{--}163\text{ }\mu\text{g RNAL}^{-1}$, and $0.03\text{--}0.06\text{ }\mu\text{g DNAL}^{-1}$ were measured, yielding $3.1\text{--}13.8\text{ nmol ATP-PL}^{-1}$, $0.6\text{--}4.5\text{ nmol PL-PL}^{-1}$, $42.2\text{--}163\text{ nmol RNA-PL}^{-1}$, and $0.06\text{--}0.13\text{ nmol DNA-PL}^{-1}$. Thus, the contribution of RNA to the DOP pool was the highest, whereas the contributions of ATP, PL, and DNA were relatively small (Table 3). The changes in all of these components over time were not related to changes in the total DOP pool (Fig. 10).

PO_4 concentrations ranged between 0.06 and $0.41\text{ }\mu\text{mol L}^{-1}$ (mean $0.21 \pm 0.09\text{ }\mu\text{mol L}^{-1}$, $n = 21$), thus comprising $24.3 \pm 11.2\%$ ($n = 21$) of the TP pool (Fig. 6). With a few exceptions, PO_4 concentrations declined from the beginning of the study period until the end of phase I and increased during phase II and the beginning of phase III. These changes were caused by upwelling of PO_4 enriched deep water of higher salinity and lower temperatures. The subsequent decline in PO_4 between days 33 and 40 was caused by the stimulation of phytoplankton production, as indicated by the increase in Chl *a* concentration (Fig. 4). For the whole experimental period, the Spearman rank correlation showed an inverse relationship between PO_4 and particulate organic matter such as Chl *a*, PC, and PN (Table 5).

3.2.4 Uptake of PO_4 and ATP

Applying [^{33}P] PO_4 , PO_4 turnover times in the fjord were in the range of 30–379 h (1.2–15 days) (mean $139 \pm 98\text{ h}$, $n = 18$) (Fig. 9a), corresponding to uptake rates of $0.73\text{--}3.37\text{ nmol L}^{-1}\text{ h}^{-1}$ (mean $1.64 \pm 0.82\text{ nmol L}^{-1}\text{ h}^{-1}$, $n = 18$) (Table 4). These rates were influenced by multiple factors, including temperature, phytoplankton biomass, and DP, POP, and PO_4 concentrations as deduced from Table 5. Despite the paucity of

BGD

12, 17543–17593, 2015

Effects of CO_2 perturbation on phosphorus pool sizes

M. Nausch et al.

Title Page

Abstract

Introduction

Conclusions

References

Tables

Figures

◀

▶

◀

▶

Back

Close

Full Screen / Esc

Printer-friendly Version

Interactive Discussion



data pairs, the total PO₄ uptake rate correlated with total BPP and with BPP in the fraction < 5 μm ($r = 0.886$; $p = 0.0188$; $n = 6$ for each relationship).

Within the experimental period, the turnover times shortened on days 15–17 (Fig. 9a), when temperature and Chl *a* (Figs. 3 and 4) reached a maximum and PO₄ concentrations were lowest (Figs. 5d). Although the shortest turnover times were expected to be coupled with the highest uptake rates, the latter were estimated 2 days later, between days 17 and 19. The day-to-day variations conformed to the small changes in temperature and PO₄ concentrations. Uptake was dominated by the size fraction < 3 μm in most of the measurements (Table 4), which accounted for 17.4–92.3 % (mean 72.2 ± 20.6 %) of the total uptake rate. The mean contribution of the size fractions > 3 μm was 27.8 ± 20.6 %. Assuming that autotrophic organisms were largely responsible for the uptake by this fraction, the specific PO₄ uptake rates of phytoplankton, calculated from the size fraction > 3 μm and the Chl *a* concentration, were 0.02 and 0.46 nmol (μg Chl *a*)⁻¹ h⁻¹.

The turnover times of ATP (7.5–62 h, or 0.3–2.6 days; mean 23 ± 15 h or 0.96 ± 0.59 days; $n = 15$) were significantly shorter than those of PO₄ (Fig. 9c), without any apparent relationship between the two. The longest ATP turnover times of 2.6 and 1.7 days occurred on days 9 and 15, respectively, when PO₄ turnover times were short. Based on measured ATP concentrations, 0.03–0.15 nmol ATP L⁻¹ h⁻¹ was converted, thus delivering 0.13–0.46 nmol P L⁻¹ h⁻¹ (Table 4). The size fraction < 3 μm utilized 85.0–97.8 % (mean 92.4 ± 4.7 %) of the ATP whereas only a small portion (2.2–15 %) could be attributed to the size fraction > 3 μm. ATP uptake rates and concentrations did not correlate with any of the other measured parameters (data not shown), with the exception that ATP turnover time correlated with BPP > 5 μm ($r = 0.943$, $p = 0.048$, $n = 6$).

BGD

12, 17543–17593, 2015

Effects of CO₂ perturbation on phosphorus pool sizes

M. Nausch et al.

Title Page

Abstract

Introduction

Conclusions

References

Tables

Figures

◀

▶

◀

▶

Back

Close

Full Screen / Esc

Printer-friendly Version

Interactive Discussion



4 Discussion

An increase in CO₂ in marine waters and the associated acidification may potentially have multiple effects on organisms and biogeochemical element cycling (Gattuso and Hansson, 2011). However, reported findings indicate wide ranging responses, probably depending on the investigated species and growth conditions. For example, CO₂ stimulation as well as lack of stimulation were found for primary production and carbon fixation (Beardall et al., 2009; Boettjer et al., 2014), DOC release (Engel et al., 2014; MacGilchrist et al., 2014) and phytoplankton growth (Riebesell and Tortell, 2011). Thus, the responses of organisms and ecosystems to enhanced CO₂ concentrations are complex and still poorly understood. The present study is the first to determine the effects of increased CO₂ levels on the phosphorus cycle in a brackish water ecosystem.

4.1 Response of P-pools and P-uptake to enhanced CO₂ in the mesocosms

The Finish side of the Gulf of Finland is one of the most important upwelling regions in the Baltic Sea. During our investigation in 2012, surface temperatures, obtained from the NOAA satellite (Siegel and Gerth, 2013) showed that upwelling persisted during the whole study period but with varying intensity. The intensity of upwelling shaped the pattern of temperature in the fjord and in the mesocosms varying from 7.8 to 15.9°C. Such variations in temperature influence the phosphorus transformation and interleave with CO₂ effects.

While nutrients were added in previous mesocosms experiments (Riebesell et al., 2008; Schulz et al., 2008), no amendments were undertaken in this study in order to be close to natural conditions. Initial PO₄ concentrations of only $0.17 \pm 0.01 \mu\text{mol L}^{-1}$ were measured, however, PO₄ was never exhausted (Figs. 5 and 6). Cellular C:P and N:P ratios were close to the Redfield ratio. Therefore, phosphorus limitation unlikely occurred in this experiment. Simultaneous low nitrate and ammonium concentrations (Paul et al., 2015b) formed nutrient conditions that benefit the growth of diazotrophic cyanobacteria. However, any cyanobacteria bloom failed to appear, despite the low-

Effects of CO₂ perturbation on phosphorus pool sizes

M. Nausch et al.

Title Page

Abstract

Introduction

Conclusions

References

Tables

Figures



Back

Close

Full Screen / Esc

Printer-friendly Version

Interactive Discussion



Effects of CO₂ perturbation on phosphorus pool sizes

M. Nausch et al.

Title Page

Abstract

Introduction

Conclusions

References

Tables

Figures

◀

▶

◀

▶

Back

Close

Full Screen / Esc

Printer-friendly Version

Interactive Discussion



level presence of *Aphanizomenon sp.* and *Anabaena sp.* (Paul et al., 2015a) as potential seed stock. For Baltic Sea summer conditions, the phytoplankton development with maximum Chl *a* concentrations of 2.2–2.5 $\mu\text{g L}^{-1}$ remained relatively low with the highest contribution of cryptophytes and chlorophytes in phase I and at the beginning of phase II. Picoplankton was mostly the dominating size fraction amounting ~ 20 – 70% of Chl *a* in phase I and rising to $\sim 85\%$ in phase III (Paul et al., 2015b). However, a positive correlation of $f\text{CO}_2$ with the Chl *a* size fraction $> 20\mu\text{m}$ was estimated. The abundance of diatoms that could be a part of this fraction increased from \sim day 23 to day 30 and might have an influence on this relationship.

Against this background, the CO₂ perturbation did not cause significant changes in phosphorus pool sizes, DOP composition, and P-uptake rates from PO₄ and ATP when the whole study period was considered. However, small but nevertheless significant, short-term effects on PO₄ and POP pool sizes were observed in phases I and III (Fig. 7). CO₂ elevation stimulated the formation of POP until day 3 (Fig. 5b) when chlorophytes, cyanobacteria, prasinophytes and the pico-cyanobacteria started to grow (Paul et al., 2015b).

The effects of CO₂ addition on PO₄ and POP pool sizes were evident from day 23 onwards (Figs. 5 and 7). PO₄ concentrations were slightly, but significantly lower in the high CO₂ treatment than in the untreated mesocosms, accompanied by significantly elevated POP concentrations indicating that the transformation of PO₄ into POP was likely stimulated under high CO₂ conditions. Since Chl *a* was elevated as well at similar POP : Chl *a* ratios, the PO₄ taken up was used for new biomass formation. However, the elevated transformation of PO₄ into POP was not detected in the PO₄ uptake rates which can be seen as gross uptake rates. Thus, it is likely that not the gross uptake but rather the net uptake was modified, e.g. via reduction in P-release from biomass under CO₂ elevation.

It is hard to assess the short-term effects that we have found in phase I. Uptake and release are assumed to be continuous processes and can alter the P pool sizes on timescales shorter than one day. Thus, variations and differences in the treatments

Effects of CO₂ perturbation on phosphorus pool sizes

M. Nausch et al.

Title Page

Abstract

Introduction

Conclusions

References

Tables

Figures

◀

▶

◀

▶

Back

Close

Full Screen / Esc

Printer-friendly Version

Interactive Discussion



can be overseen at daily sampling. Unger et al. (2013) demonstrated that an accelerated PO₄ uptake by the cyanobacterium *Nodularia spumigena* under elevated CO₂ incubations could only be observed during the first hours. Thereafter, the differences were balanced and the same level of radiotracer labeling was reached in all treatments.

5 An acceleration in formation of particulate P concentrations under CO₂ elevation without any changes of PO₄ turnover times was also observed by Tanaka et al. (2008). They observed an increase of the POP amount and an earlier appearance of the POP maximum under CO₂ elevation.

Correlations calculated by using the Spearman rank test between P pools or up-
10 take rates and other parameters for each mesocosm are presented in Table 2. The relationships between POP and TP with Chl *a* disappeared at elevated *f*CO₂, whereas correlations developed between POP and PC as well as between the PO₄ uptake by phytoplankton > 3 μm and the POP : Chl *a* ratio (Table 2). These shifts could be caused by changes in the phytoplankton composition deduced from CO₂ effects on the pigment
15 composition (Paul et al., 2015b).

Independent of the CO₂ treatment, TP decreased by 2.6 nmol L⁻¹ day⁻¹ in all meso-
cosms over the course of the experiment, in agreement with the measured sedimentation rates (Paul et al., 2015b). The strongest decrease (~ 3.2 nmol L⁻¹ day⁻¹) occurred during phase I. Of the total TP removal during this phase (48 nmol L⁻¹), 84 %
20 (~ 40.5 nmol L⁻¹) could be explained by the decrease in POP and 16 % (~ 8 nmol L⁻¹) by changes in the dissolved pool. However, the PO₄ decline (~ 34.5 nmol L⁻¹) was stronger than that of the total dissolved P pool since DOP increased in parallel by ~ 26.5 nmol L⁻¹. Thus, about 77 % of the PO₄ reduction was retrieved as DOP and remained in the dissolved P-pool being the main pathway of PO₄ transformation.

25 4.2 Phosphorus dynamics in the Storfjärden

Measurements of P-pool sizes and P uptake in the fjord provided new information about the phosphorus dynamics in a Baltic Sea upwelling system and in times when diazotrophic cyanobacteria did not dominate the phytoplankton community. Nutrient

N-limited. This may also have been the case during our study. Thus, the relatively long PO_4 turnover times might have been caused not only by low temperatures but also by the reduction in bacterioplankton activities due to C and N limitations and could be the reason that PO_4 was not depleted completely in the mesocosms and in fjord water.

5 Conclusions

Surface water in Storfjärden showed highly variable $f\text{CO}_2$ conditions and reached levels up to $800\ \mu\text{atm}$, which is similar to that expected in ca. 100 years from now. Deduced from the high frequency of upwelling events there, organisms are confronted with elevated $f\text{CO}_2$ more or less regularly and are used to high $f\text{CO}_2$ variability. This could explain the minimal response of the phytoplankton community. A general impact of $f\text{CO}_2$ on P pools and P uptake rates could not be identified for the overall period of investigation. However, temporary responses to $f\text{CO}_2$ elevation were observed for the transformation of PO_4 into POP. Although statistically significant, it is difficult to assess if the differences between the treatments are of ecological relevance. Potentially, such short-term variations are possible in the phosphorus dynamics since the transformation can take place on hourly scales and transformations are in the nanomolar concentration range. There are also indications that relationships of P pool sizes or uptake with Chl *a* and PC can change as $f\text{CO}_2$ increases. This would have an effect on biogeochemical cycles. This study also provides information on the phosphorus cycle in an upwelling-driven ecosystem of the Baltic Sea. P pool sizes were in the range characteristic for spring and cooler summers when low temperatures inhibit cyanobacteria bloom formation. The transformation of PO_4 into DOP may be the major pathway of phosphorus cycling under hydrographical and phytoplankton growth conditions as occurred in our experiment.

Acknowledgement. We are grateful to the KOSMOS team for their invaluable help with the logistics and maintenance of the mesocosms throughout the experiment. In particular, we sincerely thank Andrea Ludwig for organizing and coordinating the campaign and for the daily CTD

Effects of CO_2 perturbation on phosphorus pool sizes

M. Nausch et al.

Title Page

Abstract

Introduction

Conclusions

References

Tables

Figures

⏪

⏩

◀

▶

Back

Close

Full Screen / Esc

Printer-friendly Version

Interactive Discussion



measurements. We appreciate the assistance of Jehane Ouriqua in the nutrient analysis and that of many other participants who carried out the samplings. We also appreciate the collegial atmosphere during the work and thank everyone who contributed to it. We would also like to acknowledge the staff of the Tvärminne Zoological Station for their hospitality and support, for allowing us to use the experimental facilities, and for providing CTD data for the summers of 2008–2011. Finally, we thank Jana Woelk for analysing the phosphorus samples in the IOW. This study was funded by the BMBF project BIOACID II (FKZ 03F06550).

References

- Ammerman, J. W., Hood, R. R., Case, D., and Cotner, J. B.: Phosphorus deficiency in the Atlantic: an emerging paradigm in oceanography, *EOS*, 84, 165–170, 2003.
- Beardall, J., Stojkovic, S., and Larsen, S.: Living in a high CO₂ world: impacts of global climate change on marine phytoplankton, *Plant Ecol. Divers.*, 2, 191–205, 2009.
- Bellerby, R. G. J., Schulz, K. G., Riebesell, U., Neill, C., Nondal, G., Heegaard, E., Johannessen, T., and Brown, K. R.: Marine ecosystem community carbon and nutrient uptake stoichiometry under varying ocean acidification during the PeECE III experiment, *Biogeosciences*, 5, 1517–1527, doi:10.5194/bg-5-1517-2008, 2008.
- Bjorkman, K. M. and Karl, D. M.: A novel method for the measurement of dissolved adenosine and guanosine triphosphate in aquatic habitats: applications to marine Microb. Ecol., *J. Microbiol. Meth.*, 47, 159–167, 2001.
- Boettjer, D., Karl, D. M., Letelier, R. M., Viviani, D. A., and Church, M. J.: Experimental assessment of diazotroph responses to elevated seawater $p\text{CO}_2$ in the North Pacific Subtropical Gyre, *Global Biogeochem. Cy.*, 28, 601–616, 2014.
- Borges, A. V., Delille, B., and Frankignoulle, M.: Budgeting sinks and sources of CO₂ in the coastal ocean: diversity of ecosystems counts, *Geophys. Res. Lett.*, 32, L14601, doi:10.1029/2005GL023053, 2005.
- Caldeira, K. and Wickett, M. E.: Ocean model predictions of chemistry changes from carbon dioxide emissions to the atmosphere and ocean, *J. Geophys. Res.-Oceans*, 110, C09S04, doi:10.1029/2004JC002671, 2005.

Effects of CO₂ perturbation on phosphorus pool sizes

M. Nausch et al.

Title Page

Abstract

Introduction

Conclusions

References

Tables

Figures

◀

▶

◀

▶

Back

Close

Full Screen / Esc

Printer-friendly Version

Interactive Discussion



Effects of CO₂ perturbation on phosphorus pool sizes

M. Nausch et al.

Title Page

Abstract

Introduction

Conclusions

References

Tables

Figures



Back

Close

Full Screen / Esc

Printer-friendly Version

Interactive Discussion



Casey, J. R., Lomas, M. W., Michelou, V. K., Dyhrman, S. T., Orchard, E. D., Ammerman, J. W., and Sylvan, J. B.: Phytoplankton taxon-specific orthophosphate (Pi) and ATP utilization in the western subtropical North Atlantic, *Aquat. Microb. Ecol.*, 58, 31–44, 2009.

Clayton, T. D. and Byrne, R. H.: Spectrophotometric seawater pH measurements: total hydrogen ion concentration scale calibration of m-cresol purple and at-sea results, *Deep-Sea Res. Pt. I*, 40, 2115–2129, 1993.

Czerny, J., Barcelos e Ramos, J., and Riebesell, U.: Influence of elevated CO₂ concentrations on cell division and nitrogen fixation rates in the bloom-forming cyanobacterium *Nodularia spumigena*, *Biogeosciences*, 6, 1865–1875, doi:10.5194/bg-6-1865-2009, 2009.

Dickson, A. G., Sabine, C. L., and Christian, J. R. E.: Guide to best practices for ocean CO₂ measurements, PICES special publication 3, North Pacific Marine Science Organisation, Sidney, Canada, 191 pp., 2007.

Eichner, M., Rost, B., and Kranz, S. A.: Diversity of ocean acidification effects on marine N-2 fixers, *J. Exp. Mar. Biol. Ecol.*, 457, 199–207, 2014.

Eisler, R.: Ocean acidification, a comprehensive overview, Science Publisher, St. Helier, Jersey, British channel Islands, 252 pp., 2011.

Endres, S., Unger, J., Wannicke, N., Nausch, M., Voss, M., and Engel, A.: Response of *Nodularia spumigena* to pCO₂ – Part 2: Exudation and extracellular enzyme activities, *Biogeosciences*, 10, 567–582, doi:10.5194/bg-10-567-2013, 2013.

Engel, A., Piontek, J., Grossart, H. P., Riebesell, U., Schulz, K. G., and Sperling, M.: Impact of CO₂ enrichment on organic matter dynamics during nutrient induced coastal phytoplankton blooms, *J. Plankton Res.*, 36, 641–657, 2014.

Frommel, A. Y., Schubert, A., Piatkowski, U., and Clemmesen, C.: Egg and early larval stages of Baltic cod, *Gadus morhua*, are robust to high levels of ocean acidification, *Mar. Biol.*, 160, 1825–1834, 2013.

Gattuso, J. P. and Hansson, L. (Eds.): Ocean acidification, Oxford University Press, Oxford, 2011.

Grasshoff, K., Ehrhardt, M., and Kremling, K. (Eds.): Methods of Seawater Analysis, 2nd edition, Verlag Chemie, Weinheim, Germany, 1983.

Grossart, H. P., Allgaier, M., Passow, U., and Riebesell, U.: Testing the effect of CO₂ concentration on the dynamics of marine heterotrophic bacterioplankton, *Limnol. Oceanogr.*, 51, 1–11, 2006.

Effects of CO₂ perturbation on phosphorus pool sizes

M. Nausch et al.

Title Page

Abstract

Introduction

Conclusions

References

Tables

Figures



Back

Close

Full Screen / Esc

Printer-friendly Version

Interactive Discussion



Hiebenthal, C., Philipp, E. E. R., Eisenhauer, A., and Wahl, M.: Effects of seawater $p\text{CO}_2$ and temperature on shell growth, shell stability, condition and cellular stress of Western Baltic Sea *Mytilus edulis* (L.) and *Arctica islandica* (L.), *Mar. Biol.*, 160, 2073–2087, 2013.

IPCC, 2001: Climate Change 2001: The Scientific Basis. Third Assessment Report of the Intergovernmental Panel on Climate Change, edited by: Houghton, J. T., Ding, Y., Griggs, D. J., Noguer, M., van der Linden, P. J., Dai, X., Maskell, K., and Johnson, C. A., Cambridge University Press, Cambridge, UK and NY, USA, 82 pp., 2001.

IPCC, 2013: Climate Change 2013: The Physical Science Basis. Working Group I Contribution to the Fifth Assessment Report of the Intergovernmental Panel on Climate Change, edited by: Stocker, T. F., Qin, D., Plattner, G. K., Tignor, M. M. B., Allen, S. K., Boschung, J., Nauels, A., Xia, Y., Bex, V., and Midgley, P. M., Cambridge University Press, Cambridge, UK and NY, USA, 1535 pp., 2013.

Jeffrey, S. W. and Welschmeyer, N. A.: Spectrophotometric and fluorometric equations in common use in oceanography, in: *Phytoplankton Pigments in Oceanography*, edited by: Jeffrey, S. W., Mantoura, R. F. C., and Wright, S. W., UNESCO Publishing, Paris, 1997.

Karl, D. M.: Phosphorus, the staff of life, *Nature*, 406, 31–33, 2000.

Karl, D. M. and Bailiff, M. D.: The measurements of dissolved nucleotides in aquatic environments, *Limnol. Oceanogr.*, 34, 543–558, 1989.

Karl, D. M. and Björkman, K. M.: Dynamics of DOP, in: *Biogeochemistry of Marine Dissolved Organic Matter*, edited by: Hansell, D. A., and Carlson, C. A., Academic Press, Amsterdam, 2002.

Lass, H. U., Mohrholz, V., Nausch, G., and Siegel, H.: On phosphate pumping into the surface layer of the eastern Gotland Basin by upwelling, *J. Marine Syst.*, 80, 71–89, 2010.

Llebot, C., Spitz, Y. H., Sole, J., and Estrada, M.: The role of inorganic nutrients and dissolved organic phosphorus in the phytoplankton dynamics of a Mediterranean bay, a modeling study, *J. Marine Syst.*, 83, 192–209, 2010.

Lomas, M. W., Burke, A. L., Lomas, D. A., Bell, D. W., Shen, C., Dyhrman, S. T., and Ammerman, J. W.: Sargasso Sea phosphorus biogeochemistry: an important role for dissolved organic phosphorus (DOP), *Biogeosciences*, 7, 695–710, doi:10.5194/bg-7-695-2010, 2010.

Lovdal, T., Tanaka, T., and Thingstad, T. F.: Algal-bacterial competition for phosphorus from dissolved DNA, ATP, and orthophosphate in a mesocosm experiment, *Limnol. Oceanogr.*, 52, 1407–1419, 2007.

Effects of CO₂ perturbation on phosphorus pool sizes

M. Nausch et al.

[Title Page](#)

[Abstract](#)

[Introduction](#)

[Conclusions](#)

[References](#)

[Tables](#)

[Figures](#)

◀

▶

◀

▶

[Back](#)

[Close](#)

[Full Screen / Esc](#)

[Printer-friendly Version](#)

[Interactive Discussion](#)



MacGilchrist, G. A., Shi, T., Tyrrell, T., Richier, S., Moore, C. M., Dumousseaud, C., and Achterberg, E. P.: Effect of enhanced $p\text{CO}_2$ levels on the production of dissolved organic carbon and transparent exopolymer particles in short-term bioassay experiments, *Biogeosciences*, 11, 3695–3706, doi:10.5194/bg-11-3695-2014, 2014.

5 Michelou, V. K., Lomas, M. W., and Kirchman, D. L.: Phosphate and adenosine-5'-triphosphate uptake by cyanobacteria and heterotrophic bacteria in the Sargasso Sea, *Limnol. Oceanogr.*, 56, 323–332, 2011.

Morris, A. W. and Riley, J. P.: The determination of nitrate in sea water, *Anal. Chim. Acta*, 29, 272–279, 1963.

10 Murphy, J. and Riley, J. P.: A modified single solution method for the determination of phosphate in natural waters., *Anal. Chim. Acta*, 27, 31–36, 1962.

Nausch, M. and Nausch, G.: Dissolved phosphorus in the Baltic Sea – occurrence and relevance, *J. Marine Syst.*, 87, 37–46, 2011.

15 Nausch, M., Nausch, G., and Wasmund, N.: Phosphorus dynamics during the transition from nitrogen to phosphate limitation in the central Baltic Sea, *Mar. Ecol.-Prog. Ser.*, 266, 15–25, 2004.

Nausch, M., Nausch, G., Lass, H. U., Mohrholz, V., Nagel, K., Siegel, H., and Wasmund, N.: Phosphorus input by upwelling in the eastern Gotland Basin (Baltic Sea) in summer and its effects on filamentous cyanobacteria, *Estuar. Coast. Shelf S.*, 83, 434–442, 2009.

20 Nausch, M., Nausch, G., Mohrholz, V., Siegel, H., and Wasmund, N.: Is growth of filamentous cyanobacteria supported by phosphate uptake below the thermocline?, *Estuar. Coast. Shelf S.*, 99, 50–60, 2012.

Nawrocki, M. P. and Karl, D. M.: Dissolved ATP turnover in the Bransfield Strait, Antarctica during a spring bloom, *Mar. Ecol.-Prog. Ser.*, 57, 35–44, 1989.

25 Orr, J. C.: Recent and future changes in ocean carbonate chemistry, in: *Ocean Acidification*, edited by: Guttaso, J. P., and Hansson, L., Oxford University Press, NY, USA, 41–66, 2011.

Pajusalu, L., Martin, G., and Pollumae, A.: Results of laboratory and field experiments of the direct effect of increasing CO₂ on net primary production of macroalgal species in brackish-water ecosystems, *P. Est. Acad. Sci.*, 62, 148–154, 2013.

30 Pansch, C., Nasrolahi, A., Appelhans, Y. S., and Wahl, M.: Impacts of ocean warming and acidification on the larval development of the barnacle *Amphibalanus improvisus*, *J. Exp. Mar. Biol. Ecol.*, 420, 48–55, 2012.

Effects of CO₂ perturbation on phosphorus pool sizes

M. Nausch et al.

[Title Page](#)

[Abstract](#)

[Introduction](#)

[Conclusions](#)

[References](#)

[Tables](#)

[Figures](#)



[Back](#)

[Close](#)

[Full Screen / Esc](#)

[Printer-friendly Version](#)

[Interactive Discussion](#)



Patey, M. D., Rijkenberg, M. J. A., Statham, P. J., Stinchcombe, M. C., Achterberg, E. P., and Mowlem, M.: Determination of nitrate and phosphate in seawater at nanomolar concentrations, *Trac-Trend. Anal. Chem.*, 27, 169–182, 2008.

Paul, A. J., Achterberg, E. P., Bach, L. T., Boxhammer, T., Czerny, J., Haunost, M., Schulz, K.-G., Stühr, A., and Riebesell, U.: No observed effect of ocean acidification on nitrogen biogeochemistry in a summer Baltic Sea plankton community, *Biogeochemistry*, submitted, 2015a.

Paul, A. J., Bach, L. T., Schulz, K.-G., Boxhammer, T., Czerny, J., Achterberg, E. P., Hellemann, D., Trense, Y., Nausch, M., Sswat, M., and Riebesell, U.: Effect of elevated CO₂ on organic matter pools and fluxes in a summer, post spring-bloom Baltic Sea plankton community, *Biogeosciences Discuss.*, 12, 6863–6927, doi:10.5194/bgd-12-6863-2015, 2015b.

Pierrot, L., D. and Wallace, D.: MS Excel program developed for CO₂ system calculations, Carbon Dioxide Information Analysis Center, Oak Ridge National Laboratory, US Department of Energy, Oak Ridge, Tennessee, http://cdiac.ornl.gov/ftp/co2sys/CO2SYS_calc_XLS_v2.1/ (last access: October 2014), 2006.

Riebesell, U. and Tortell, P.: Effects of ocean acidification on pelagic organisms and ecosystems, in: *Ocean Acidification*, edited by: Gattuso, J. P., and Hansson, L., Oxford University Press, NY, USA, 2011.

Riebesell, U., Bellerby, R. G. J., Grossart, H.-P., and Thingstad, F.: Mesocosm CO₂ perturbation studies: from organism to community level, *Biogeosciences*, 5, 1157–1164, doi:10.5194/bg-5-1157-2008, 2008.

Riebesell, U., Czerny, J., von Bröckel, K., Boxhammer, T., Büdenbender, J., Deckelnick, M., Fischer, M., Hoffmann, D., Krug, S. A., Lentz, U., Ludwig, A., Mücke, R., and Schulz, K. G.: Technical Note: A mobile sea-going mesocosm system – new opportunities for ocean change research, *Biogeosciences*, 10, 1835–1847, doi:10.5194/bg-10-1835-2013, 2013.

Riemann, L., Holmfeldt, K., and Titelman, J.: Importance of Viral Lysis and Dissolved DNA for Bacterioplankton Activity in a P-Limited Estuary, Northern Baltic Sea, *Microb. Ecol.*, 57, 286–294, 2009.

Rossoll, D., Sommer, U., and Winder, M.: Community interactions dampen acidification effects in a coastal plankton system, *Mar. Ecol.-Prog. Ser.*, 486, 37–46, 2013.

Sanudo-Wilhelmy, S. A., Kustka, A. B., Gobler, C. J., Hutchins, D. A., Yang, M., Lwiza, K., Burns, J., Capone, D. G., Raven, J. A., and Carpenter, E. J.: Phosphorus limitation of nitrogen fixation by *Trichodesmium* in the central Atlantic Ocean, *Nature*, 411, 66–69, 2001.

Effects of CO₂ perturbation on phosphorus pool sizes

M. Nausch et al.

Title Page

Abstract

Introduction

Conclusions

References

Tables

Figures



Back

Close

Full Screen / Esc

Printer-friendly Version

Interactive Discussion



- Schulz, K. G. and Riebesell, U.: Diurnal changes in seawater carbonate chemistry speciation at increasing atmospheric carbon dioxide, *Mar. Biol.*, 160, 1889–1899, 2013.
- Schulz, K. G., Riebesell, U., Bellerby, R. G. J., Biswas, H., Meyerhöfer, M., Müller, M. N., Egge, J. K., Neijstgaard, J. C., Neill, C., Wohlers, J., and Zöllner, E.: Build-up and decline of organic matter during PeECE III, *Biogeosciences*, 5, 707–718, doi:10.5194/bg-5-707-2008, 2008.
- Siegel, H. and Gerth, M.: Sea surface temperature in the Baltic Sea in 2012, HELCOM Baltic Sea environment fact sheets, <http://www.helcom.fi/baltic-sea-trends/environment-fact-sheets> (last access: May 2015), 2013.
- Simon, M. and Azam, F.: Protein content and protein synthesis rates of planktonic marine bacteria, *Mar. Ecol.-Prog. Ser.*, 51, 201–213, 1989.
- Siuda, W. and Chrost, R. J.: Utilization of selected dissolved organic phosphorus compounds by bacteria in lake water under non-limiting orthophosphate conditions, *Pol. J. Environ. Stud.*, 10, 475–483, 2001.
- Stemmer, K., Nehrke, G., and Brey, T.: Elevated CO₂ Levels do not Affect the Shell Structure of the Bivalve *Arctica islandica* from the Western Baltic, *PLoS ONE*, 8, doi:10.1371/journal.pone.0070106, 2013.
- Suzumura, M.: Phospholipids in marine environments: a review, *Talanta*, 66, 422–434, 2005.
- Suzumura, M. and Ingall, E. D.: Concentrations of lipid phosphorus and its abundance in dissolved and particulate organic phosphorus in coastal seawater, *Mar. Chem.*, 75, 141–149, 2001.
- Suzumura, M. and Ingall, E. D.: Distribution and dynamics of various forms of phosphorus in seawater: insight from field observation in the Pacific Ocean and a laboratory experiment, *Science direct: Deep-Sea Res. Pt. I*, 51, 1113–1130, 2004.
- Tanaka, T., Thingstad, T. F., Løvdal, T., Grossart, H.-P., Larsen, A., Allgaier, M., Meyerhöfer, M., Schulz, K. G., Wohlers, J., Zöllner, E., and Riebesell, U.: Availability of phosphate for phytoplankton and bacteria and of glucose for bacteria at different *p*CO₂ levels in a mesocosm study, *Biogeosciences*, 5, 669–678, doi:10.5194/bg-5-669-2008, 2008.
- Tyrrell, T.: The relative influences of nitrogen and phosphorus on oceanic primary production, *Nature*, 400, 525–531, 1999.
- Unger, J., Endres, S., Wannicke, N., Engel, A., Voss, M., Nausch, G., and Nausch, M.: Response of *Nodularia spumigena* to *p*CO₂ – Part 3: Turnover of phosphorus compounds, *Biogeosciences*, 10, 1483–1499, doi:10.5194/bg-10-1483-2013, 2013.

Vehmaa, A., Brutemark, A., and Engstrom-Ost, J.: Maternal Effects May Act as an Adaptation Mechanism for Copepods Facing pH and Temperature Changes, *PLoS ONE*, 7, doi:10.1371/journal.pone.0048538, 2012.

5 Wannicke, N., Endres, S., Engel, A., Grossart, H.-P., Nausch, M., Unger, J., and Voss, M.: Response of *Nodularia spumigena* to $p\text{CO}_2$ – Part 1: Growth, production and nitrogen cycling, *Biogeosciences*, 9, 2973–2988, doi:10.5194/bg-9-2973-2012, 2012.

BGD

12, 17543–17593, 2015

Effects of CO_2 perturbation on phosphorus pool sizes

M. Nausch et al.

Title Page

Abstract

Introduction

Conclusions

References

Tables

Figures



Back

Close

Full Screen / Esc

Printer-friendly Version

Interactive Discussion



Effects of CO₂ perturbation on phosphorus pool sizes

M. Nausch et al.

Title Page

Abstract

Introduction

Conclusions

References

Tables

Figures

◀

▶

◀

▶

Back

Close

Full Screen / Esc

Printer-friendly Version

Interactive Discussion



Table 1. Minimum, maximum and mean values of hydrographical parameters and $f\text{CO}_2$ for the different phases in the fjord. Temperatures in the mesocosms were identical with those in surrounding fjord water.

phase	min	max	mean
water temperature (°C)			
0	7.82	8.71	8.20
I	9.66	15.86	12.27
II	7.89	14.79	11.68
III	8.35	12.61	10.83
salinity			
0	5.72	5.85	5.78
I	5.46	5.85	5.65
II	5.67	6.04	5.82
III	5.9	6.05	5.98
pH			
0	8.09	8.23	8.16
I	8.11	8.30	8.17
II	7.81	8.30	8.00
III	7.75	7.93	7.83
$f\text{CO}_2$ (µatm)			
0	250	347	298
I	207	336	283
II	208	679	465
III	521	800	668

Effects of CO₂ perturbation on phosphorus pool sizes

M. Nausch et al.

Table 4. PO₄- and ATP uptake rates in the fjord and in the mesocosms. Minimum, maximum and mean values as well as the contribution of the size fraction < 3 μm to the total activity are given for the whole period of investigation (each: *n* = 16 for PO₄ and *n* = 6 for ATP uptake).

fCO ₂ (μatm)	total PO ₄ uptake (nmol L ⁻¹ h ⁻¹)			portion (%) < 3 μm	total ATP-P uptake (nmol L ⁻¹ h ⁻¹)			portion (%) < 3 μm
	min	max	mean		min	max	mean	
Fjord	0.87	2.81	1.63 ± 0.58	76 ± 15	0.04	0.51	0.26 ± 0.15	92 ± 5
365	0.82	3.89	1.67 ± 0.82	81 ± 11	0.14	1.08	0.43 ± 0.33	96 ± 2
368	0.65	2.74	1.61 ± 0.58	86 ± 7	0.16	0.97	0.47 ± 0.27	96 ± 2
497	0.61	3.03	1.52 ± 0.59	86 ± 6	0.20	1.07	0.54 ± 0.28	96 ± 2
821	0.91	2.83	1.60 ± 0.59	88 ± 8	0.14	0.71	0.36 ± 0.21	97 ± 2
1003	0.67	3.79	1.73 ± 0.85	86 ± 6	0.22	0.69	0.39 ± 0.15	97 ± 1
1231	0.87	2.23	1.53 ± 0.43	87 ± 6	0.17	0.67	0.44 ± 0.17	97 ± 2

Title Page

Abstract

Introduction

Conclusions

References

Tables

Figures

⏪

⏩

◀

▶

Back

Close

Full Screen / Esc

Printer-friendly Version

Interactive Discussion



Effects of CO₂ perturbation on phosphorus pool sizes

M. Nausch et al.

Table 5. Significance level (p) deduced from of Spearman Rank correlations that were calculated between the parameters in fjord water listed in the table.

Variable	T	S	$f\text{CO}_2$	PO_4	POP	DOP	$\text{Chl } a$	PC	C/P
T (°C)		0.0001 ⁻	0.0061 ⁻	< 0.0001 ⁻	< 0.0001 ⁺	n.s.	< 0.0001 ⁺	0.0083 ⁺	n.s.
S	0.0001 ⁻		< 0.0001 ⁺	< 0.0001 ⁺	0.0030 ⁻	0.0445 ⁻	< 0.0001 ⁻	< 0.0001 ⁻	0.0181 ⁻
$p\text{CO}_2$	0.0061 ⁻	< 0.0001 ⁺		< 0.0001 ⁺	0.0288 ⁻	n.s.	< 0.0001 ⁻	< 0.0001 ⁻	0.0104 ⁻
PO_4 ($\mu\text{mol L}^{-1}$)	< 0.0001 ⁻	< 0.0001 ⁺	< 0.0001 ⁺		< 0.0001 ⁻	0.0049 ⁻	< 0.0001 ⁻	0.0008 ⁻	n.s.
POP ($\mu\text{mol L}^{-1}$)	< 0.0001 ⁺	0.0030 ⁻	0.0288 ⁻	< 0.0001 ⁻		0.0345 ⁺	< 0.0001 ⁺	0.0016 ⁺	n.s.
DOP ($\mu\text{mol L}^{-1}$)	n.s.	0.0445 ⁻	n.s.	0.0049 ⁻	0.0345 ⁺		0.0271 ⁺	n.s.	n.s.
$\text{Chl } a$ ($\mu\text{g L}^{-1}$)	< 0.0001 ⁺	< 0.0001 ⁻	< 0.0001 ⁻	< 0.0001 ⁻	< 0.0001 ⁺	0.0271 ⁺		0.0003 ⁺	n.s.
PC ($\mu\text{mol L}^{-1}$)	0.0083 ⁺	< 0.0001 ⁻	< 0.0001 ⁻	0.0008 ⁻	0.0016 ⁺	n.s.	0.0003 ⁺		0.0014 ⁺
PN ($\mu\text{mol L}^{-1}$)	0.0007 ⁺	< 0.0001 ⁻	< 0.0001 ⁻	0.0001 ⁻	< 0.0001 ⁺	n.s.	< 0.0001 ⁺	< 0.0001 ⁺	0.0156 ⁺
C/P	n.s.	0.0181 ⁻	0.0104 ⁻	n.s.	n.s.	n.s.	n.s.	0.0014 ⁺	
PO_4 -TO time (d)	0.0001 ⁻	< 0.0001 ⁺	0.0250 ⁺	< 0.0001 ⁺	0.0048 ⁻	0.0099 ⁺	0.0006 ⁻	n.s.	n.s.
PO_4 total uptake ($\text{nmol L}^{-1}\text{h}^{-1}$)	n.s.	0.0244 ⁻	0.0403 ⁻	0.0455 ⁻	n.s.	n.s.	n.s.	n.s.	n.s.
PO_4 uptake > 3 μm ($\text{nmol L}^{-1}\text{h}^{-1}$)	n.s.	0.0284 ⁻	0.0006 ⁻	n.s.	n.s.	n.s.	n.s.	0.0386 ⁺	n.s.
PO_4 uptake < 3 μm ($\text{nmol L}^{-1}\text{h}^{-1}$)	n.s.	n.s.	n.s.	n.s.	n.s.	n.s.	n.s.	n.s.	n.s.
BBP total ($\mu\text{g C L}^{-1}\text{h}^{-1}$)	0.0005 ⁺	0.0037 ⁻	n.s.	0.0018 ⁻	0.0022 ⁺	n.s.	< 0.0001 ⁺	0.0092 ⁺	n.s.
BBP > 5 μm ($\mu\text{g C L}^{-1}\text{h}^{-1}$)	0.0088 ⁺	0.0370 ⁻	n.s.	0.0353 ⁻	0.0056 ⁺	n.s.	0.0027 ⁺	0.0479 ⁺	n.s.
BBP 0.2–5 μm ($\mu\text{g C L}^{-1}\text{h}^{-1}$)	0.0012 ⁺	0.0072 ⁻	n.s.	0.0041 ⁻	0.0102 ⁺	n.s.	< 0.0001 ⁺	0.0114 ⁺	n.s.

Title Page

Abstract

Introduction

Conclusions

References

Tables

Figures

⏪

⏩

◀

▶

Back

Close

Full Screen / Esc

Printer-friendly Version

Interactive Discussion



Effects of CO₂ perturbation on phosphorus pool sizes

M. Nausch et al.

Title Page

Abstract

Introduction

Conclusions

References

Tables

Figures

⏪

⏩

◀

▶

Back

Close

Full Screen / Esc

Printer-friendly Version

Interactive Discussion



Table 5. Continued.

Variable	PO ₄ TO-time	total PO ₄ uptake	> 3μm PO ₄ uptake	< 3μm PO ₄ uptake	total BPP	> 5μm BPP	0.2–5μm BPP
<i>T</i> (°C)	0.0001 ⁻	n.s.	n.s.	n.s.	0.0005 ⁺	0.0088 ⁺	0.0012 ⁺
<i>S</i>	< 0.0001 ⁺	0.0244 ⁻	0.0284 ⁻	n.s.	0.0037 ⁻	0.0370 ⁻	0.0072 ⁻
<i>p</i> CO ₂	0.0250 ⁺	0.0403 ⁻	0.0006 ⁻	n.s.	n.s.	n.s.	n.s.
PO ₄ (μmol L ⁻¹)	< 0.0001 ⁺	0.0455 ⁻	n.s.	n.s.	0.0018 ⁻	0.0353 ⁻	0.0041 ⁻
POP (μmol L ⁻¹)	0.0048 ⁻	n.s.	n.s.	n.s.	0.0022 ⁺	0.0056 ⁺	0.0102 ⁺
DOP (μmol L ⁻¹)	0.0099 ⁺	n.s.	n.s.	n.s.	n.s.	n.s.	n.s.
Chl <i>a</i> (μg L ⁻¹)	0.0006 ⁻	n.s.	n.s.	n.s.	< 0.0001 ⁺	0.0027 ⁺	< 0.0001 ⁺
PC (μmol L ⁻¹)	n.s.	n.s.	0.0386 ⁺	n.s.	0.0092 ⁺	0.0479 ⁺	0.0114 ⁺
PN (μmol L ⁻¹)	0.0165 ⁻	n.s.	n.s.	n.s.	0.0092 ⁺	0.0479 ⁺	0.0114 ⁺
C/P	n.s.	n.s.	n.s.	n.s.	n.s.	n.s.	n.s.
PO ₄ -TO time (d)	< 0.0001 ⁻	< 0.0001 ⁻	n.s.	n.s.	n.s.	n.s.	n.s.
PO ₄ total uptake (nmol L ⁻¹ h ⁻¹)	< 0.0001 ⁻	n.s.	n.s.	n.s.	0.0188 ⁺	n.s.	0.0188 ⁺
PO ₄ uptake > 3μm (nmol L ⁻¹ h ⁻¹)	n.s.	n.s.	n.s.	n.s.	n.s.	n.s.	n.s.
PO ₄ uptake < 3μm (nmol L ⁻¹ h ⁻¹)	n.s.	n.s.	n.s.	n.s.	n.s.	n.s.	n.s.
BBP total (μg CL ⁻¹ h ⁻¹)	n.s.	0.0188 ⁺	n.s.	n.s.	< 0.0001 ⁺	< 0.0001 ⁺	< 0.0001 ⁺
BPP > 5μm (μg CL ⁻¹ h ⁻¹)	n.s.	n.s.	n.s.	n.s.	< 0.0001 ⁺	< 0.0001 ⁺	0.0001 ⁺
BPP 0.2–5μm (μg CL ⁻¹ h ⁻¹)	n.s.	0.0188 ⁺	n.s.	n.s.	< 0.0001 ⁺	0.0001 ⁺	

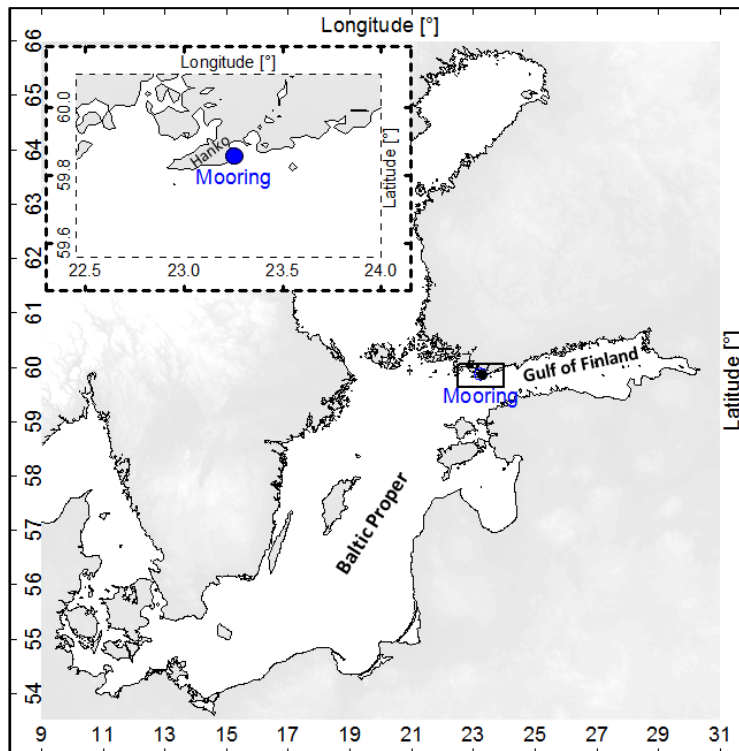


Figure 1. The Baltic Sea and the location near the peninsula Hango in the western Gulf of Finland where the mesocosms were deployed.

Effects of CO₂ perturbation on phosphorus pool sizes

M. Nausch et al.

Title Page	
Abstract	Introduction
Conclusions	References
Tables	Figures
◀	▶
◀	▶
Back	Close
Full Screen / Esc	
Printer-friendly Version	
Interactive Discussion	



Effects of CO₂ perturbation on phosphorus pool sizes

M. Nausch et al.

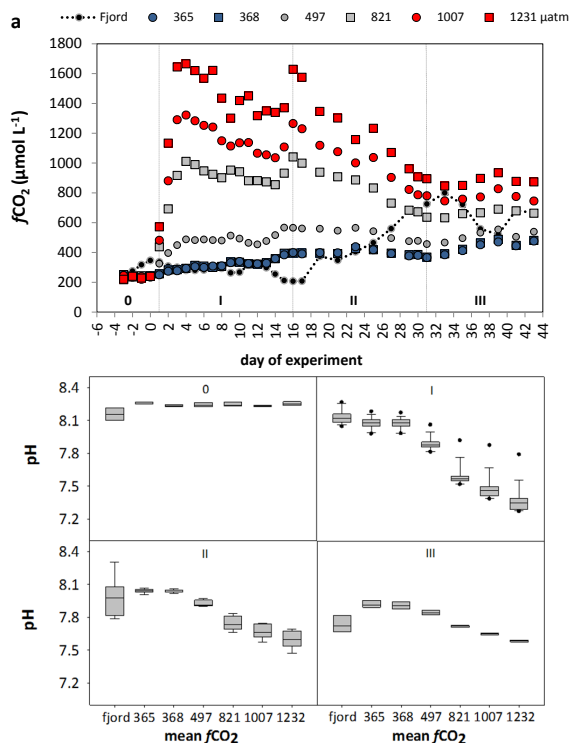


Figure 2. (a) $f\text{CO}_2$ values in the mesocosms and in the fjord throughout the experiment. Small black dots show the $f\text{CO}_2$ in the ambient fjord water. Treatment of the mesocosms with CO₂ saturated fjord water at the beginning of the experiment (days 0–4) created different $f\text{CO}_2$ levels in the mesocosms: blue symbols represents the untreated mesocosms, grey the intermediate, and red the high CO₂ treated mesocosms. The treatment was repeated at day 16. (b) Corresponding pH ranges in the mesocosms during the four phases. Despite decreasing trend over time, a gradient between the mesocosms was kept over the whole period.

Effects of CO₂ perturbation on phosphorus pool sizes

M. Nausch et al.

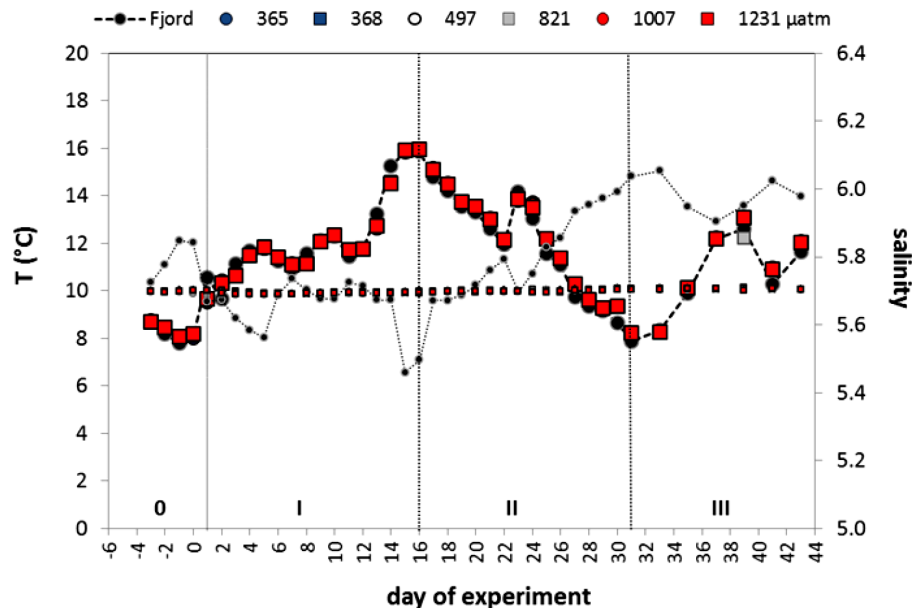


Figure 3. Temperature and salinity averaged over the 17 m surface layer of the mesocosms and the fjord. The data were obtained from daily CTD casts. Large symbols represent temperature and the small symbols salinity. Fjord water is shown as black dots with broken line while blue symbols denote untreated, grey intermediate and red high $f\text{CO}_2$ levels in the mesocosms. According to the temperature regime, the experimental period can be divided into four phases (phases 0, I, II and III).

Effects of CO₂ perturbation on phosphorus pool sizes

M. Nausch et al.

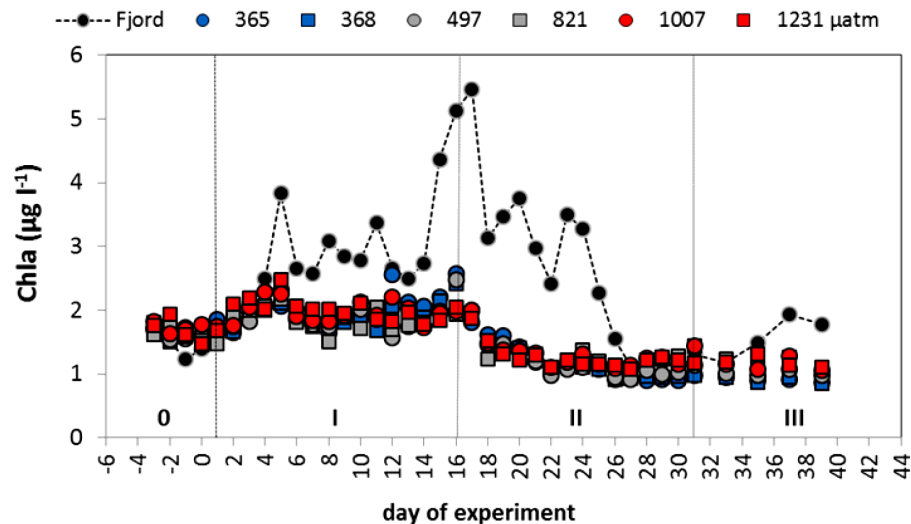


Figure 4. Chl *a* concentrations in fjord water and in the mesocosms with different $f\text{CO}_2$ conditions. The development over time can be divided into three phases as well. Blue represent untreated, grey intermediate, and red highly treated $f\text{CO}_2$ levels. Black dots are the Chl *a* concentrations in the fjord water.

[Title Page](#)
[Abstract](#)
[Introduction](#)
[Conclusions](#)
[References](#)
[Tables](#)
[Figures](#)
[◀](#)
[▶](#)
[◀](#)
[▶](#)
[Back](#)
[Close](#)
[Full Screen / Esc](#)
[Printer-friendly Version](#)
[Interactive Discussion](#)


Effects of CO₂ perturbation on phosphorus pool sizes

M. Nausch et al.

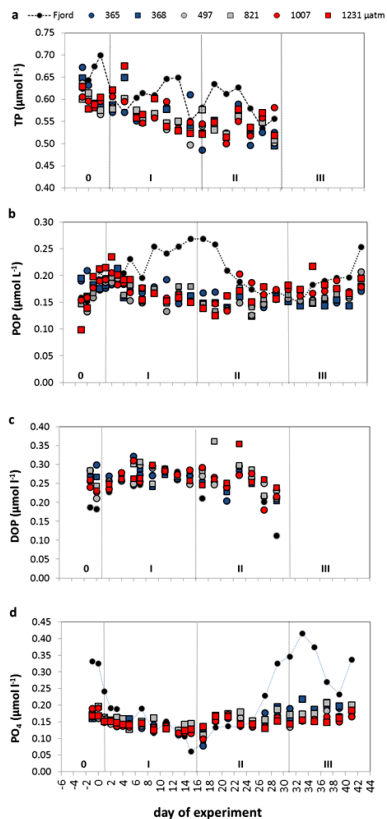


Figure 5. (a–d) Development of total phosphorus (TP) and the three measured P-fractions in fjord water (black dots with dotted line) and in the mesocosms over time. Blue represents untreated, grey intermediate and red high $f\text{CO}_2$ treatment levels.

[Title Page](#)
[Abstract](#)
[Introduction](#)
[Conclusions](#)
[References](#)
[Tables](#)
[Figures](#)
[⏪](#)
[⏩](#)
[◀](#)
[▶](#)
[Back](#)
[Close](#)
[Full Screen / Esc](#)
[Printer-friendly Version](#)
[Interactive Discussion](#)


Effects of CO₂ perturbation on phosphorus pool sizes

M. Nausch et al.

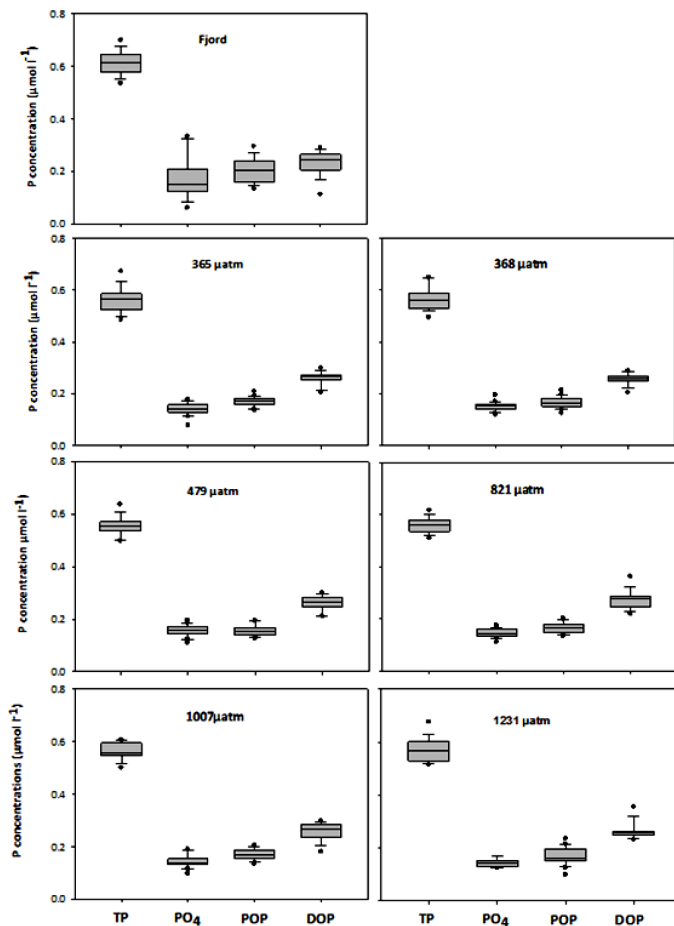


Figure 6. Contribution of the individual P-fractions to TP in fjord water and in the respective mesocosms. The data are averaged for the period when TP measurements were done (day –3–day 29).

Title Page

Abstract

Introduction

Conclusions

References

Tables

Figures

◀

▶

◀

▶

Back

Close

Full Screen / Esc

Printer-friendly Version

Interactive Discussion



Effects of CO₂ perturbation on phosphorus pool sizes

M. Nausch et al.

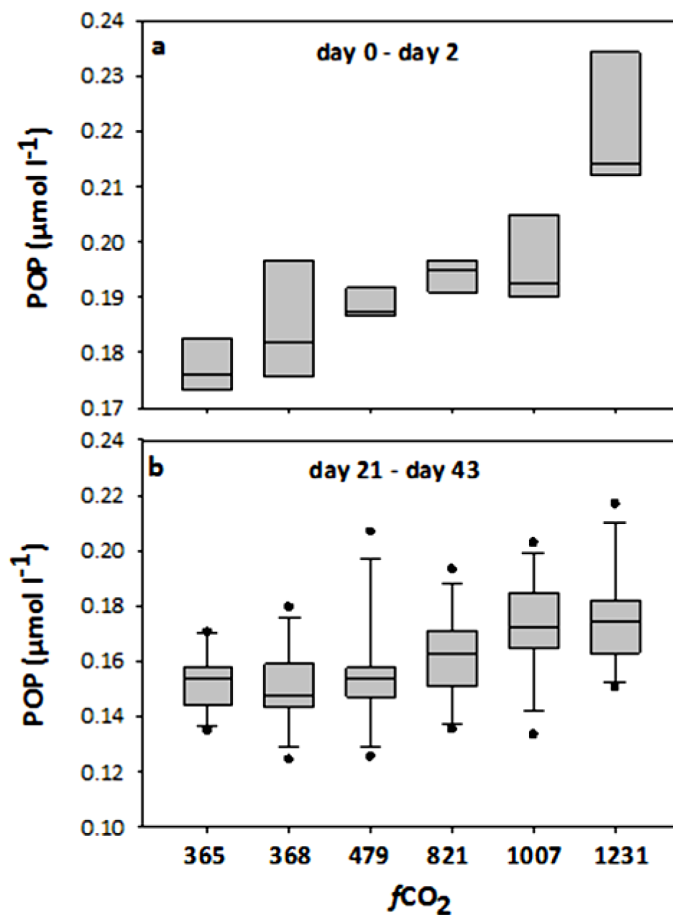


Figure 7. POP concentration in the mesocosms during the initial phase from day 0 to day 2 (a) and from day 23 until the end (b) of experiment.

[Title Page](#)[Abstract](#)[Introduction](#)[Conclusions](#)[References](#)[Tables](#)[Figures](#)[◀](#)[▶](#)[◀](#)[▶](#)[Back](#)[Close](#)[Full Screen / Esc](#)[Printer-friendly Version](#)[Interactive Discussion](#)

Effects of CO₂ perturbation on phosphorus pool sizes

M. Nausch et al.

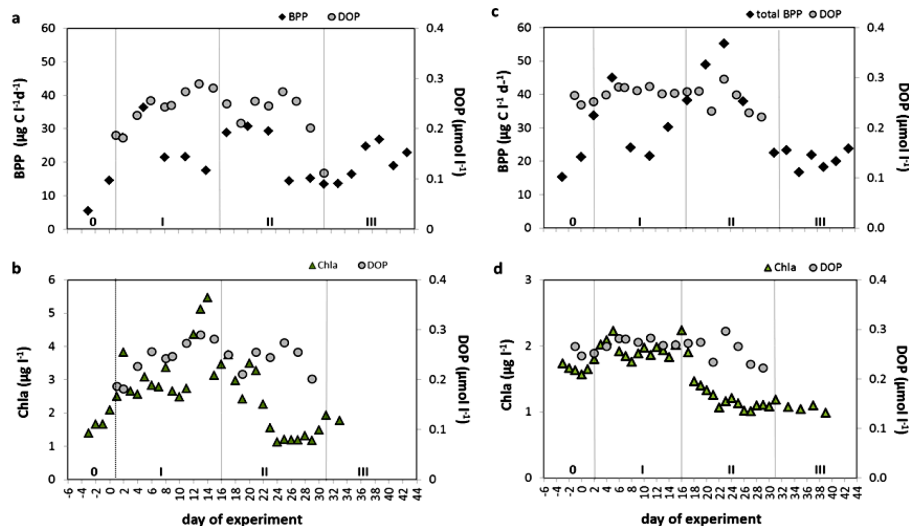


Figure 8. Development of DOP in relation to bacterial production (BPP) and phytoplankton biomass (Chl *a*) in the fjord (**a**, **b**) and in the mesocosms (**c**, **d**). For mesocosms, mean values averaged over all treatments are given.

Title Page

Abstract

Introduction

Conclusions

References

Tables

Figures

◀

▶

◀

▶

Back

Close

Full Screen / Esc

Printer-friendly Version

Interactive Discussion



Effects of CO₂ perturbation on phosphorus pool sizes

M. Nausch et al.

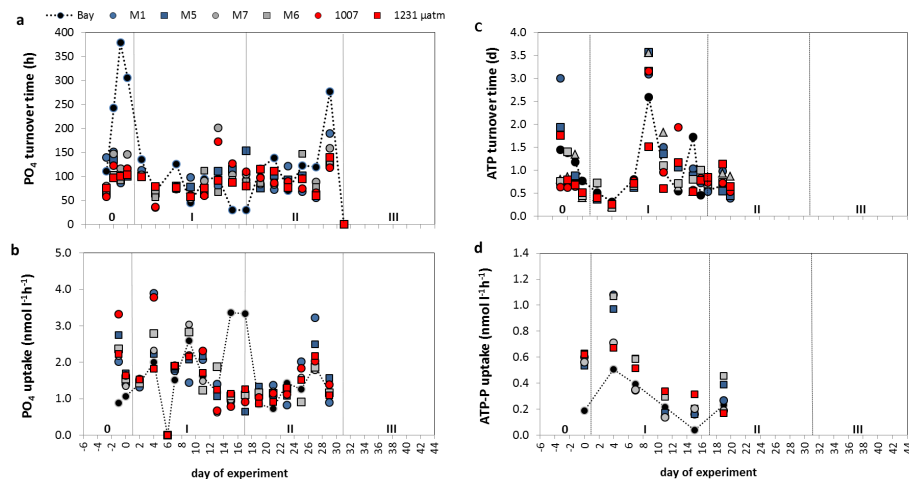


Figure 9. Turnover times of PO₄ (a) and ATP (c) in fjord water and in the mesocosms as well as the respective uptake rates (b, d).

Title Page

Abstract

Introduction

Conclusions

References

Tables

Figures



Back

Close

Full Screen / Esc

Printer-friendly Version

Interactive Discussion



Effects of CO₂ perturbation on phosphorus pool sizes

M. Nausch et al.

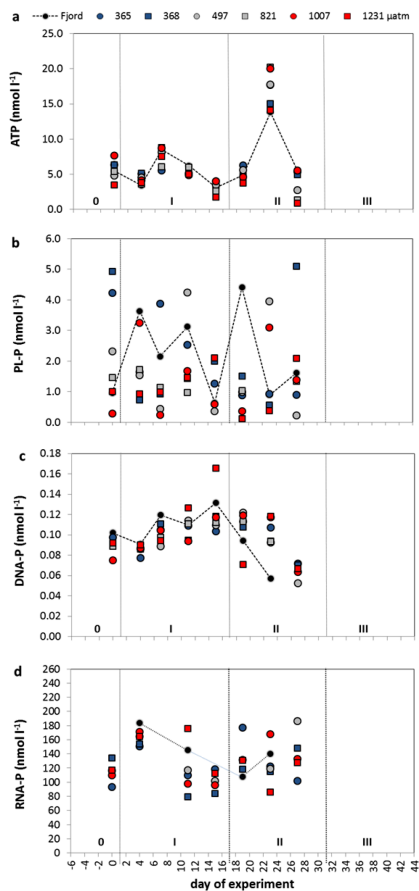


Figure 10. Development of DOP compounds in the mesocosms and in the fjord from day 0 to day 27.

Title Page

Abstract

Introduction

Conclusions

References

Tables

Figures



Back

Close

Full Screen / Esc

Printer-friendly Version

Interactive Discussion

